https://doi.org/10.17221/197/2023-CJFS

Assessing essential oil composition in *Cinnamomum cassia* leaves from different regions of China using GC-MS and FTIR spectroscopy

Yan Huang[1], Yujie Liu[1], Huiping Tan[1], Yanrong Cheng[1], Kunyang Tao[1], Dingze Gu[1], Huaizu Cai[1], Chengjie Li[1], Kaiyi Guo[1], Cheng Wu[1], Hong Wu[1,2], Yanqun Li[1,2]**

[1]*Guangdong Key Laboratory for Innovative Development and Utilization of Forest Plant Germplasm, South China Agricultural University, Guangzhou, China*

[2]*Medicinal Plants Research Center, South China Agricultural University, Guangzhou, China*

**Corresponding authors: wh@scau.edu.cn; liyanqun@scau.edu.cn*

Yan Huang and Yujie Liu contributed equally to this work.

Citation: Huang Y., Liu Y., Tan H., Cheng Y., Tao K., Gu D., Cai H., Li C., Guo K., Wu C., Wu H., Li Y. (2024): Assessing essential oil composition in *Cinnamomum cassia* leaves from different regions of China using GC-MS and FTIR spectroscopy. Czech J. Food Sci., 42: 141–152.

Abstract: In this study, volatile compounds from *Cinnamomum cassia* Presl. leaves from different regions of China were identified using gas chromatography coupled with mass spectrometry (GC-MS) and Fourier-transform infrared (FTIR) spectroscopy combined with chemometrics. The results showed that the essential oil yields greatly varied across regions, with the density of oil cells at the accumulation and saturation stages playing a key role in this yield. GC-MS analysis revealed a higher content of *trans*-cinnamaldehyde in samples from the Xijiang River basin (No. 1–8) than in those from Baise Guangxi (No. 9). Variable importance in projection analysis identified five differential marker components for assessing the geographical origin of *C. cassia* leaves: *trans*-cinnamaldehyde, acetophenone, *cis*-cinnamaldehyde, camphor, and α-thujene. Hierarchical cluster analysis, similarity evaluation, and principal component analysis from FTIR fingerprinting indicated that essential oil compositions of samples No. 1–6 from the Xijiang River basin were closely related. In contrast, the Baise sample (Western Guangxi) significantly differed from the other eight, likely due to the geographical distance. Our results indicate that the methods employed are effective for determining the geographical distribution and assessing the quality of raw cinnamon in herbal medicine.

Keywords: chemometrics; oil cells; composition analysis; quality evaluation

Cinnamomum cassia Presl., a member of the *Lauraceae* family, is a widely grown traditional herbal medicine in various tropical and subtropical regions, including Guangdong, Guangxi, Fujian, Taiwan, and Yunnan. Approximately 80% of the world's cinnamon oil, a yellow or yellow-brown liquid, comes

Supported by the GuangDong Basic and Applied Basic Research Foundation, China (Project No. 2020B1515420007), by the Nature Science Foundation of China (Project No. 32370383), and by the Open Competition Program of Ten Major Directions of Agricultural Science and Technology Innovation for the 14th Five-Year Plan of Guangdong Province, China (Project No. 2022SDZG07).

https://doi.org/10.17221/197/2023-CJFS

from Guangxi and Guangdong. Extracted from dried bark, branches, and leaves of *C. cassia,* the oil's quality is mainly determined by its *trans*-cinnamaldehyde content, an important quality index (China Pharmacopeia Commission 2020). Rich in terpenoids and aromatic compounds, the oil of *C. cassia* has numerous beneficial properties, including antidiabetic, anti-inflammatory, antioxidant, antiulcer, anti-allergic, anticancer, and antibacterial effects (Muhammad and Dewettinck 2017; Farag et al. 2022). As a plant-derived product, this oil is often used in food as an additive, condiment, and flavoring agent.

Currently, the bark of *C. cassis* is the main source of commercial cassia raw materials (Shen et al. 2012). With increased demand due to the wider utilisation of *C. cassia* oil, other parts of the plant, such as leaves, rich in essential oil, are being used as additional resources and also used in medicine, food flavouring, and preservatives (Błaszczyk et al. 2021). Compared to bark and twigs, cassia leaves regenerate faster, are abundant, and are cost-effective but underused. Therefore, optimising the utilisation of cassia leaves can enhance cinnamon resource efficiency and conservation.

However, various factors affect the chemical composition of essential oils, such as individual genetic variation, different parts, growth stages and environmental changes (Li et al. 2020; Thinh and Thin 2023). The accumulation of secondary metabolites is highly dependent on environmental factors such as light, temperature, growing location, soil water, soil fertility, and salinity (Jan et al. 2021). It has been reported that different geographical locations greatly affect the content and composition of essential oil in cinnamon bark and branches (Li et al. 2013a; Cen et al. 2016). Studies have investigated volatile compounds in cassia leaves, focusing on variations due to different growth ages (Li et al. 2013b) and species (Bai et al. 2021), providing valuable data for evaluating and utilising cassia leaf resources. Unfortunately, the essential oil yield and chemical composition from different locations of cassia leaves remain unknown. This study analyses the chemical composition of the essential oil of *C. cassia* leaves from different regions using gas chromatography-mass spectrometry (GC-MS) and Fourier-transform infrared (FTIR) spectroscopy combined with chemometrics. Our results provide a practical guide for the rapid determination and quality evaluation of various types of cassia oil and a scientific basis for evaluating and rationally using cinnamon plants.

MATERIAL AND METHODS

Plant materials. Samples of cassia leaves were collected 2019 from *C. cassia* species in the main cinnamon-producing areas of the Guangxi and Guangdong provinces and identified by Professor Rongjing Zhang (South China Agricultural University, Guangzhou, China). Voucher specimens were deposited in the herbarium of the Department of Botany at the South China Agricultural University (for details see Table 1).

The preparation of *Cinnamomum cassia* powder. Fresh leaves of *C. cassia* were randomly collected. Each sample contained leaves from three plants. The samples were washed with tap water, air-dried till uniform weight (about 15 days) at room temperature, ground into 60-mesh powder, and stored in a drying oven.

Extraction of the essential oils. Essential oils were isolated as previously described (Li et al. 2013a). The yields of the essential oils were determined in triplicate, and the results were expressed as mean values. Analysis of variance (ANOVA) was performed, and plots were obtained using Origin software (version 8.0); P-levels < 0.05 were considered statistically significant.

Gas chromatography-mass spectrometry analysis. GC-MS analysis was conducted on a 7890A gas chromatograph with a 5975C Plus mass spectrometer (Agilent, United States). Separated using a fused silica capillary Agilent Technology HP-5 MS column with 5% phenyl methyl siloxane (30 m × 0.25 mm inner diameter, 0.1 μm film thickness). Injector and detector temperatures were 150 and 200 °C, respectively. The column temperature was initially 100 °C for 4 min, then increased to 130 °C at 5 °C·min^{-1} and maintained for 20 min. The carrier gas, high-purity helium, had a linear velocity of 1.2 mL·min^{-1} at a 30:1 split ratio. Electron ionisation was used as the ionisation method, with the ion source temperature set at 230 °C. The mass spectrometer scanned a mass range of 30–550 atomic mass units (AMU) at 1-sec intervals. The essential oil of each sample was prepared with dichloromethane to a concentration of 10 mg·mL^{-1}, and 1.0 μL of this solution was introduced into the system for analysis.

Some volatile compounds were identified by co-elution with authentic standards and the NIST05 mass spectra on an HP-MSD chemical workstation (National Institute of Standards and Technology, USA) and corroborated with relevant literature. Quantitative analyses of each essential oil component (expressed as area percentage) were carried out using GC-MS peak area normalisation, with results as mean values from three injections per sample.

https://doi.org/10.17221/197/2023-CJFS

Table 1. Cinnamon species and collection sites

Sample No.	Location	Age	Longitude and latitude	Average temperature (°C)	Annual precipitation (mm)	Soil type
1	Aicun, Gaoyao, Guangdong, China	13	112.388039°E 23.157942°N	20.79	1 671.4	lateritic red
2	Fuhao, Deqing, Guangdong, China	12	111.987411°E 23.154303°N	20.79	1 671.4	lateritic red
3	South China Agricultural University, Guangdong, China	12	113.364723°E 23.159725°N	22.63	1 736.1	grey fluvoaquic
4	Xinli, Wuzhou, Guangxi, China	14	111.249219°E 23.414137°N	21.90	1 544.9	lateritic red
5	Huanglin, Cenxi, Guangxi, China	12	111.325981°E 22.879412°N	21.90	1 544.9	lateritic red
6	Longxu, Wuzhou, Guangxi, China	12	111.252441°E 23.367392°N	21.90	1 544.9	lateritic red
7	Songshan, Yulin, Guangxi, China	12	110.491463°E 22.933722°N	22.88	1 405.7	lateritic red
8	Kangtang, Yulin, Guangxi, China	11	110.531532°E 22.950361°N	22.88	1 405.7	lateritic red
9	Nongan, Baise, Guangxi, China	11	106.247658°E 23.449732°N	22.80	1 070.7	calcareous

Fourier-transform infrared spectroscopy. An FTIR spectrometer (Nicolet 5700; Thermo Nicolet Corp., USA) was equipped with a deuterated triglycine sulfate detector. Spectra were recorded from 400 to 4 000 cm^{-1} at a resolution of 4 cm^{-1}, a temperature of 25 °C, and 30% relative air humidity. A quantity of 200 mg dried potassium bromide (KBr) powder was accurately weighed to create two transparent blank KBr tablets, each approximately 5 mm in diameter and 1 mm thick. Two microliters of the essential oil of the cinnamon sample were sandwiched between these tablets to form a thin liquid film for infrared (IR) spectroscopy. Five samples were prepared for each region, with four random sweeps per sample, yielding 20 spectra. The final sample spectrum was the average, with background, H_2O, and carbon dioxide (CO_2) interference subtracted. Raw spectral data were baseline corrected and smoothed using OMNIC software (version 8.0) before undergoing standard normal variate processing in Unscrambler software (version 9.7).

Orthogonal partial least squares-discriminant analysis (OPLS-DA). The relative percent areas of common peaks in the GC-MS fingerprint profiles of *C. cassia* samples from different regions were processed with SIMCA software (version 14.1) for OPLS-DA, determining the predicted variable importance in projection (VIP).

Similarity evaluation. The correlation coefficient (r_{con}) between samples' fingerprints was calculated using the included cosine angle. The two pieces of the spectrum (the two-dimensional vector) were calculated and formulated as follows:

$$r_{con} = \frac{\sum_{i=1}^{num} x_i y_i}{\left(\sum_{i=1}^{num} (x_i)^2\right)^{\frac{1}{2}} \left(\sum_{i=1}^{num} (y_i)^2\right)^{\frac{1}{2}}} \quad (1)$$

The formula determines the directional cosine between two infrared spectra where x_i and y_i represent the intensity values of the IR spectra of two samples, denoted as x and y, at the i^{th} variable. Fingerprint profiles were evaluated for similarity using SPSS software (version 18.0).

Principal component analysis (PCA). PCA was conducted based on the singular value decomposition of the data array of the FTIR fingerprints. The first several PCA scores were used to create a projection

https://doi.org/10.17221/197/2023-CJFS

diagram, enabling visual identification of fingerprint similarities. PCA was performed using Unscrambler software.

Preparation of the semi-thin sections. The mid-tissue of mature leaves with normal growth and development was cut into 1 × 1 × 0.5 mm pieces and quickly immersed in 2.5% paraformaldehyde – 3.0% glutaraldehyde fixative [prepared in 0.1 mol·L^{-1} phosphate-buffered saline (PBS), pH 7.2]. The leaf blade was observed using the semi-thin sections method (Li et al. 2013b).

Density of the oil cells. The distribution of oil cells was determined using the tissue-clearing method and Li et al. (2013b) described. The oil cell density (N·mm^{-2}) was calculated as an average from 15 samples.

RESULTS

Distribution and developmental characteristics of oil cells in cassia leaves. Oil cells, found in roots, stems, fruits, and leaves of the plants from the *Lauraceae* family, are primary sites for essential oil biosynthesis, secretion, and storage (Li et al. 2013b; Cen et al. 2021). These oil cells, larger than the surrounding parenchyma cells, were predominantly in the sponge tissue (Figure 1A). Most cells' degraded cytoplasm and nucleus suggest that they were at a late stage of development (Figure 1A).

The modified whole tissue clearing method reported by Li et al. (2013b) was used to observe morphological characteristics of oil cells. The morphological changes during oil production, formation, and accumulation were observed (Figure 1B–C), oil cell development could be divided into five stages: oilless, formation, accumulation, saturation, and degradation (Figure 1a–e). These stages show that oil droplets are the largest and essential oil accumulation is the highest during the accumulation and saturation stages (Figure 1c and 1d). The oil droplets started degrading at the degradation stage, darkening to black (Figure 1e). So in this study, the oil cell densities were counted at the accumulation and saturation stages characterised by the highest oil concentration (Figure 2B). Sample No. 5 had the highest oil cell density (4.8 N·mm^{-2}) at the accumulation and saturation stages, followed by sample No. 6 at 4.10 N·mm^{-2}, while samples No. 7 and 8 had the lowest oil cell densities of 2.86 and 2.93 N·mm^{-2}, respectively.

Yields of essential oil analysis. The yield of essential oils extracted from *C. cassia* leaf samples via hy-

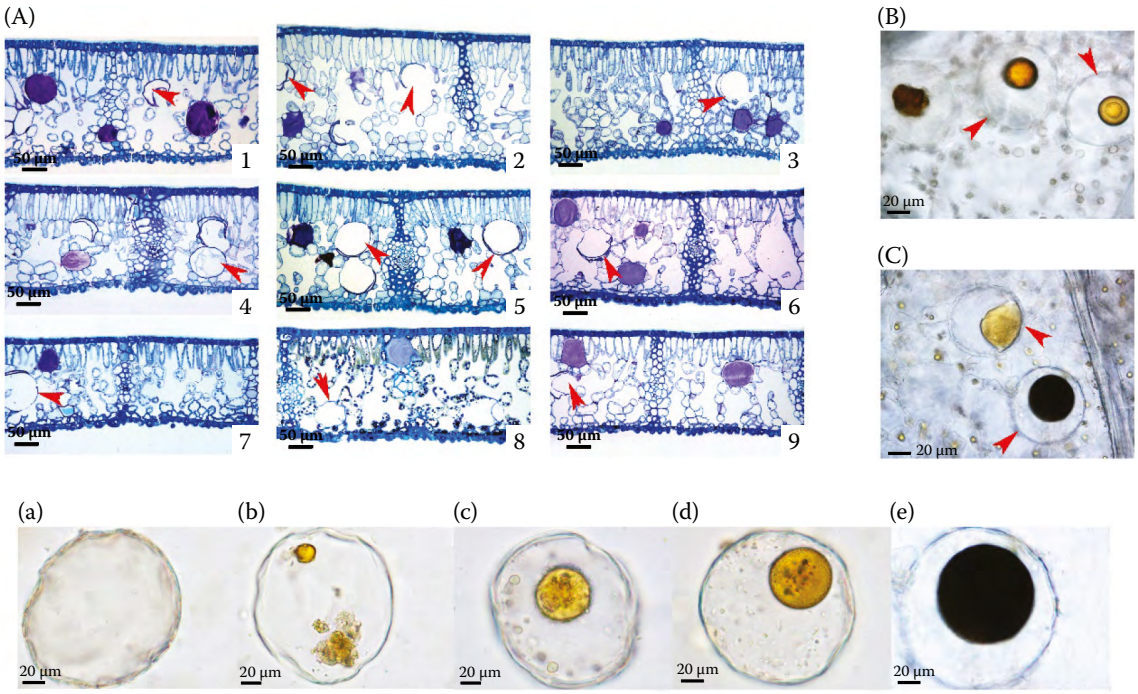

Figure 1. (A) Transverse section of a leaf, the distribution of oil cells in cassia leaves from nine samples (1–9); (B–C) observation of the dynamic process of essential oil in the oil cells of cassia leaves using improved tissue clearing method; (a) oilless stage; (b) oil at formation stage; (c) oil at accumulation stage; (d) oil at saturation stage; (e) oil at degradation stage

Arrows showing oil cells

https://doi.org/10.17221/197/2023-CJFS

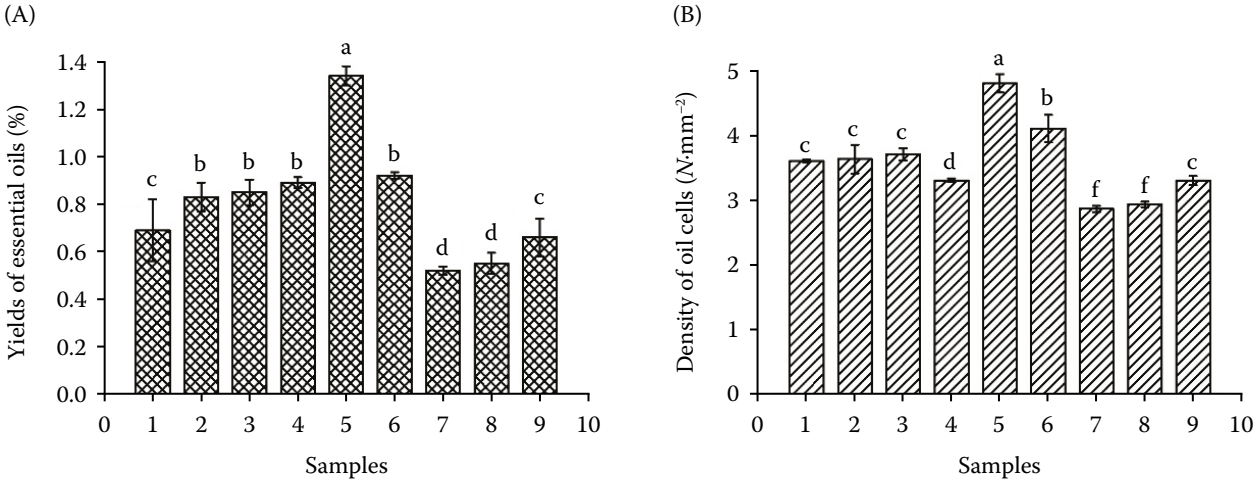

Figure 2. (A) Yields (% *w*/*w* dry basis) of essential oils of different cinnamon leaves from different regions and (B) the oil density at the accumulation and saturation stages from different regions

a–f – the columns having different lowercase letters are significantly different ($P < 0.05$)

drodistillation varied greatly between regions, ranging from 0.51 to 1.34% (Figure 2A). The highest yield was 1.34% from sample No. 5, followed by No. 6 (0.92%), No. 4 (0.89%), No. 3 (0.85%), and No. 2 (0.83%). The lowest yields were from samples No. 7 and 8 from Rongxian County at 0.51% and 0.55%, respectively.

Gas chromatography-mass spectrometry analysis of essential oil from leaves of *Cinnamomum cassia* of different regions. The chemical composition of essential oils is influenced by many factors, including genetic and environmental factors, developmental stages, formation sites, and extraction methods (Li et al. 2020). In this study, the typical GC-MS profile of the essential oils from the twig of cinnamon plants is shown in the Electronic Supplementary Material (ESM, Figure S1). Thirteen common peaks, consisting of 34 components, were identified in all samples, representing 80.05–95.54% of the total oils (Table 2). The most abundant component was *trans*-cinnamaldehyde (54.76–65.91%). The analysis showed that volatile compounds were different in different regions. For example, *trans*-cinnamaldehyde content was higher in Guangdong (60.65–65.91%) compared to Guangxi (50.36–60.38%). Additionally, other compounds like ethylbenzene (3.32–5.78%), styrene (2.44–5.91%), α-thujene (2.14–7.76%), cedrene (1.98–5.80%), acetophenone (1.61–8.21%), camphor (1.47–3.76%), and benzaldehyde (0.81–1.43%) were also found in varying amounts. Samples No. 1 and 2 had high benzaldehyde content, at 1.43% and 1.32%, respectively, while samples No. 3, 4, 5, 8, and 9 contained little to no benzaldehyde.

An orthogonal partial least square discriminant analysis (OPLS-DA) was developed using the 13 common components as *y*-variables and different regions as *x*-variables. The model fit indices were $R^2_X = 0.502$ and $R^2_Y = 0.917$, while the model prediction index (Q^2) was 0.874. Values of the coefficient of determination (R^2) and Q^2 exceeding 0.5 indicate acceptable model fit results (Yun et al. 2021). The OPLS-DA (Figure 3A) effectively differentiated samples from different regions. Thus it could be used for region identification of *C. cassia*. VIP values were derived from the thirteen common peaks and then ranked (Figure 3B). The results demonstrated that the VIP values for peaks C14 (*trans*-cinnamaldehyde), C5 (acetophenone), C13 (*cis*-cinnamaldehyde), C8 (camphor), and C3 (α-thujene) exceeded 1.0. This suggests that these five components can serve as distinctive markers for determining the geographical origin of cinnamon.

Fourier-transform infrared fingerprints of essential oils. Essential oil, a complex mix, was analysed using FTIR spectroscopy to provide structural evidence and information about functional groups. This study recorded spectra from 400 to 4 000 cm^{-1} (ESM, Figure S2). The IR characteristic fingerprint peaks for the cinnamon samples are mostly 1 800–600 cm^{-1} (Figure 4A). As illustrated in Figure 4A, the FTIR fingerprints of the nine samples share many similar peaks within the 1 800–600 cm^{-1} range of the infrared characteristic absorption spectra. Several features were extracted from the typical spectrum of *C. cassia* presented in Figure 4B. Thus, the dominant strong

Czech Journal of Food Sciences, 42, 2024 (3): 141–152

https://doi.org/10.17221/197/2023-CJFS

Table 2. Chemical compositions of *Cinnamomum cassia* essential oils from different regions

No.	Compound	*RI*	Relative content (%)									Identification
			1	2	3	4	5	6	7	8	9	
C1	ethylbenzene	856	3.32 ± 0.04^{c}	–	tr	–	4.57 ± 0.04^{b}	5.78 ± 0.14^{a}	–	–	–	GC–MS, RI
C2	styrene	866	3.16 ± 0.09^{d}	2.54 ± 0.09^{e}	4.02 ± 0.04^{c}	2.44 ± 0.03^{e}	2.61 ± 0.03^{e}	4.67 ± 0.14^{b}	5.91 ± 0.05^{a}	3.11 ± 0.02^{d}	3.09 ± 0.03^{d}	GC–MS, RI
C3	α-thujene	930	2.16 ± 0.06^{g}	2.14 ± 0.05^{g}	4.05 ± 0.09^{c}	4.67 ± 0.11^{b}	3.13 ± 0.03^{f}	3.47 ± 0.04^{e}	7.76 ± 0.19^{a}	3.04 ± 0.02^{f}	3.86 ± 0.05^{d}	GC–MS, RI
C4	benzaldehyde	988	1.43 ± 0.02^{a}	1.32 ± 0.03^{a}	–	tr	–	1.21 ± 0.04^{c}	0.81 ± 0.06^{d}	–	–	GC–MS, RI
C5	acetophenone	992	5.79 ± 0.14^{b}	2.79 ± 0.08^{f}	8.21 ± 0.25^{a}	2.06 ± 0.09^{g}	1.61 ± 0.04^{h}	4.79 ± 0.09^{c}	4.17 ± 0.06^{d}	1.70 ± 0.04^{h}	4.27 ± 0.07^{e}	GC–MS, RI
C6	α-ocimene	1 048	1.05 ± 0.01^{c}	0.46 ± 0.03^{d}	1.73 ± 0.04^{a}	–	0.96 ± 0.02^{c}	0.95 ± 0.04	1.23 ± 0.05^{b}	–	1.25 ± 0.04^{b}	GC–MS, RI
C7	β-pinene	1 092	0.80 ± 0.02^{b}	0.31 ± 0.02^{d}	–	0.88 ± 0.08^{b}	0.50 ± 0.03^{c}	0.89 ± 0.04^{b}	0.68 ± 0.04^{c}	–	1.06 ± 0.08^{a}	GC–MS, RI
C8	camphor	1 118	3.76 ± 0.09^{a}	2.23 ± 0.07^{b}	2.17 ± 0.06^{b}	1.47 ± 0.06^{e}	2.36 ± 0.04^{b}	1.78 ± 0.03^{d}	2.07 ± 0.03^{c}	2.18 ± 0.04^{b}	2.34 ± 0.05^{b}	GC–MS, RI
C9	benzenepropanal	1 162	0.51 ± 0.06^{a}	–	–	–	0.65 ± 0.02^{a}	–	tr	0.43 ± 0.03^{bc}	0.34 ± 0.02^{c}	GC–MS, RI
C10	α-terpineol	1 176	–	–	–	0.63 ± 0.02^{a}	0.36 ± 0.03^{b}	–	0.43 ± 0.04^{b}	tr	–	GC–MS, RI
C11	2,2,4-trimethyl-1,3-pentanediol	1 185	0.57 ± 0.06^{c}	0.92 ± 0.06^{a}	tr	0.38 ± 0.01^{c}	0.80 ± 0.02^{ab}	0.45 ± 0.01^{c}	0.91 ± 0.03^{a}	0.86 ± 0.04^{a}	0.31 ± 0.01^{c}	GC–MS, RI
C12	methylbutyraldehyde	1 201	0.91 ± 0.06^{a}	0.40 ± 0.03^{c}	0.20 ± 0.01^{d}	0.67 ± 0.03^{b}	0.59 ± 0.04^{b}	0.32 ± 0.02^{c}	0.49 ± 0.06^{c}	0.56 ± 0.04^{b}	0.55 ± 0.03^{b}	GC–MS, RI
C13	*cis*-cinnamaldehyde	1 215	0.36 ± 0.01^{d}	0.32 ± 0.02^{d}	tr	1.02 ± 0.07^{b}	0.45 ± 0.02^{c}	1.17 ± 0.12^{a}	0.47 ± 0.04^{c}	1.26 ± 0.08^{a}	tr	GC–MS, RI
C14	*trans*-cinnamaldehyde	1 230	60.65 ± 0.41^{b}	65.91 ± 0.94^{a}	65.57 ± 0.34^{a}	58.40 ± 0.38^{c}	60.38 ± 0.49^{b}	57.76 ± 0.14^{c}	58.45 ± 0.50^{c}	58.27 ± 0.17^{c}	50.36 ± 0.34^{d}	GC–MS, RI, Co
C15	cinnamyl acetate	1 337	0.39 ± 0.03^{d}	0.59 ± 0.02^{c}	0.58 ± 0.04^{c}	0.55 ± 0.03^{c}	0.40 ± 0.04^{d}	–	tr	0.97 ± 0.03^{a}	0.78 ± 0.06^{b}	GC–MS, RI
C16	eugenol	1 356	0.45 ± 0.02^{b}	0.45 ± 0.05^{b}	0.45 ± 0.04^{b}	0.74 ± 0.05^{a}	0.56 ± 0.03^{b}	tr	0.28 ± 0.04^{c}	0.57 ± 0.03^{b}	0.38 ± 0.03^{bc}	GC–MS, RI
C17	δ-selinene	1 364	0.47 ± 0.08^{a}	0.37 ± 0.06^{b}	–	0.51 ± 0.03^{a}	–	0.29 ± 0.04^{c}	–	0.49 ± 0.02^{a}	–	GC–MS, RI
C18	copaene	1 369	0.57 ± 0.06^{b}	0.78 ± 0.09^{a}	0.33 ± 0.02^{c}	–	–	0.30 ± 0.03^{c}	0.31 ± 0.02^{c}	0.57 ± 0.04^{b}	0.58 ± 0.04^{b}	GC–MS, RI
C19	geranyl acetate	1 373	–	0.88 ± 0.06^{a}	0.72 ± 0.07^{b}	0.17 ± 0.01^{e}	–	–	0.49 ± 0.06^{c}	0.74 ± 0.10^{b}	0.35 ± 0.03^{d}	GC–MS, RI

https://doi.org/10.17221/197/2023-CJFS

Table 2. To be continued

No.	Compound	*RI*	Relative content (%)									Identification
			1	2	3	4	5	6	7	8	9	
C20	caryophyllene	1 387	tr	1.25 ± 0.11^{a}	0.38 ± 0.03^{d}	0.63 ± 0.05^{c}	0.82 ± 0.06^{b}	0.76 ± 0.04^{b}	0.83 ± 0.05^{b}	0.79 ± 0.08^{b}	0.75 ± 0.06^{b}	GC–MS, RI
C21	isoledene	1 396	tr	0.31 ± 0.01^{c}	0.57 ± 0.02^{b}	0.63 ± 0.06^{b}	0.82 ± 0.07^{a}	0.67 ± 0.03^{b}	0.27 ± 0.01^{c}	0.62 ± 0.01^{b}	tr	GC–MS, RI
C22	cinnamic acid ethyl ester	1 432	–	–	0.57 ± 0.03^{a}	–	0.50 ± 0.02a	–	tr	–	–	GC–MS, RI, Co
C23	α-farnesene	1 435	0.36 ± 0.04^{c}	0.46 ± 0.02^{b}	0.63 ± 0.03^{a}	0.48 ± 0.07^{b}	0.42 ± 0.06^{b}	0.37 ± 0.03^{c}	0.49 ± 0.01^{b}	0.50 ± 0.03^{b}	0.31 ± 0.07^{c}	GC–MS, RI
C24	isoamyl benzoate	1 437	0.54 ± 0.03^{b}	0.82 ± 0.04^{a}	–	tr	0.35 ± 0.06^{c}	0.34 ± 0.02^{c}	–	–	0.47 ± 0.02^{b}	GC–MS, RI
C25	α-muurolene	1 455	0.42 ± 0.05^{d}	–	1.97 ± 0.12^{a}	–	0.63 ± 0.02^{c}	0.41 ± 0.06^{d}	0.75 ± 0.04^{b}	–	0.62 ± 0.06^{c}	GC–MS, RI
C26	α-bisabolol	1 465	–	0.39 ± 0.02^{c}	0.38 ± 0.06^{c}	–	0.87 ± 0.09^{a}	0.46 ± 0.04^{bc}	0.52 ± 0.06^{b}	0.67 ± 0.04^{b}	0.34 ± 0.08^{c}	GC–MS, RI
C27	cedrene	1 482	5.80 ± 0.08^{a}	1.98 ± 0.08^{h}	2.52 ± 0.18^{f}	3.29 ± 0.11^{d}	2.80 ± 0.16^{e}	2.19 ± 0.09^{g}	2.45 ± 0.12^{f}	3.93 ± 0.16^{b}	3.70 ± 0.12^{c}	GC–MS, RI
C28	α-guaiene	1 499	0.40 ± 0.02^{c}	0.40 ± 0.06^{c}	0.64 ± 0.04^{a}	0.52 ± 0.07^{b}	0.58 ± 0.06^{a}	–	0.39 ± 0.04^{c}	0.61 ± 0.06^{a}	–	GC–MS, RI
C29	o-methoxycinnamaldehyde	1 512	0.50 ± 0.06^{b}	tr	–	0.49 ± 0.08^{b}	0.42 ± 0.04^{b}	–	0.35 ± 0.03^{c}	0.65 ± 0.03^{a}	–	GC–MS, RI
C30	α-cadinene	1 536	0.47 ± 0.03^{a}	–	0.42 ± 0.08^{a}	–	0.48 ± 0.04^{a}	–	0.31 ± 0.01^{b}	–	0.38 ± 0.01^{a}	GC–MS, RI
C31	α-cadinol	1 550	0.35 ± 0.03^{b}	–	0.32 ± 0.04^{b}	0.50 ± 0.07^{a}	–	–	tr	–	–	GC–MS, RI
C32	α-calacorene	1 560	0.35 ± 0.03^{c}	–	0.43 ± 0.02^{b}	0.45 ± 0.04^{b}	tr	0.44 ± 0.06^{b}	0.37 ± 0.04^{c}	0.53 ± 0.04^{b}	1.59 ± 0.08^{a}	GC–MS, RI
Total			95.54	88.02	96.86	81.58	88.62	93.47	91.19	83.05	77.68	

$^{a–h}$ Letters in upper index are significantly different ($P < 0.05$); *RI* – retention indices based on a homologous series of normal alkanes (C5–C25); GC-MS – gas chromatography-mass spectrometry; values are expressed as mean ± SD; '–' – not detected; tr – trace, relative content < 0.1%

https://doi.org/10.17221/197/2023-CJFS

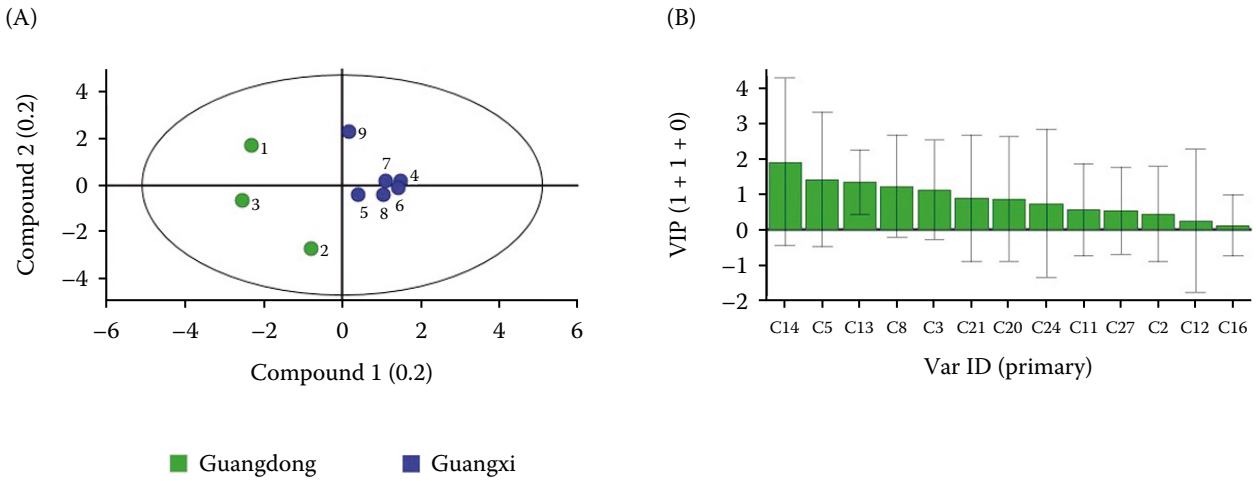

Figure 3. (A) Orthogonal partial least squares-discriminant analysis score plot and (B) variable importance in projection (VIP) diagram of *Cinnamomum cassia* from different regions

ID – thirteen common peaks

and broad peaks at 1 675 and 1 626 cm^{-1} correspond to aldehyde carbonyl C=O stretching vibration, which is consistent with the high content of cinnamaldehyde and other aldehydes in the essential oil. The peak at 1 450 cm^{-1} corresponds to the bending vibration absorption of an alcohol C-OH moiety; the one at 1 248 cm^{-1} indicates the presence of the aromatic acid ester C-O-C symmetric expansion and phenolic C-OH groups, while the peak at 1 124 cm^{-1} is associated with C-O stretch vibration. The peak at 973 cm^{-1} is assigned to the bending vibration absorption of C-H. Our results match with cinnamon bark oil FTIR data (Li et al. 2013a), indicating the chemical complexity and diversity of the essential oil of cinnamon (Figure 4).

Cluster analysis and similarity analysis of Fourier-transform infrared fingerprint of *Cinnamomum cassia* leaves. *C. cassia* leaf samples from nine locations underwent cluster and similarity analysis for their chemical composition. As shown in Figure 5A, these samples were divided into three clusters. Samples No. 1–6 clustered together, with samples No. 1–3 (from Guangdong province) forming a subcluster. These samples, from Guangdong (samples No. 1–3) and Guangxi (samples No. 4–6) provinces, share similar climatic and soil environments due to their location in the Xijiang River basin, reflected in their similar chemical compositions. Samples No. 7 and 8 (Yulin, Guangxi) formed another cluster, while sample No. 9 (Baise, Guangxi) stood as a single cluster. The similarity anal-

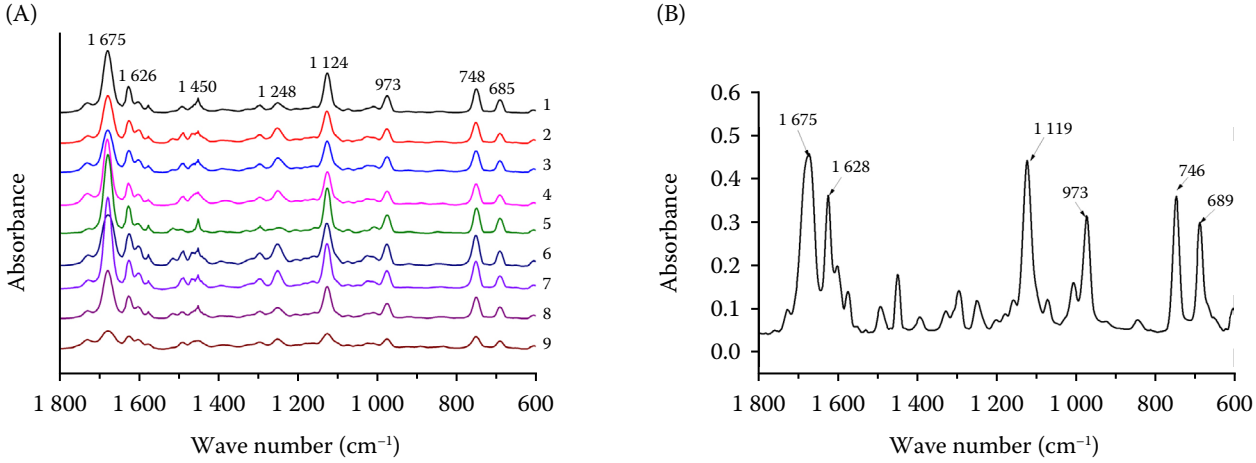

Figure 4. (A) Infrared spectra of essential oils from nine samples and (B) the typical infrared spectra of *Cinnamomum cassia*

https://doi.org/10.17221/197/2023-CJFS

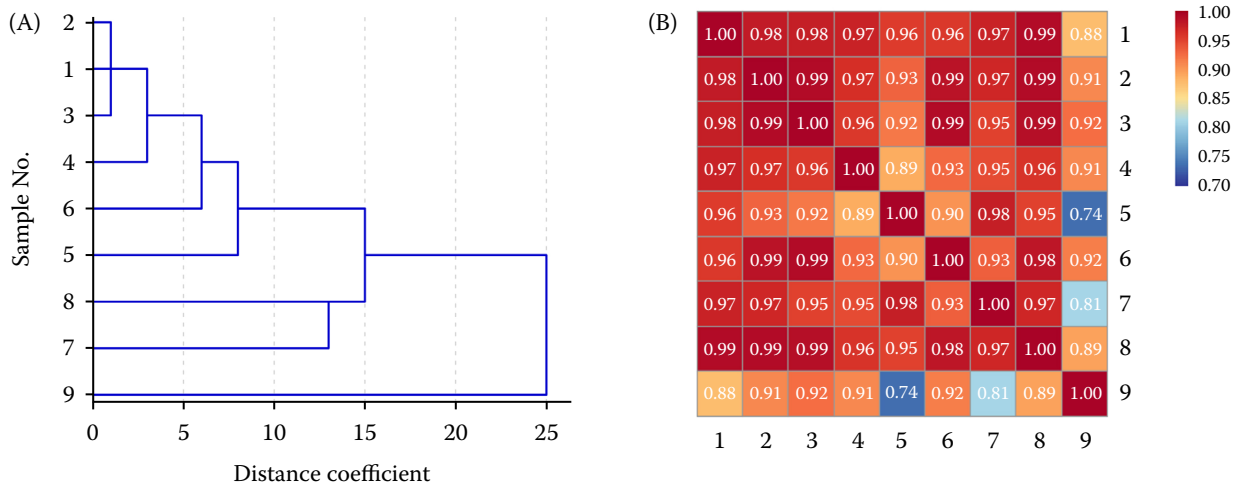

Figure 5. (A) Rescaled distance cluster combine and (B) similarity analysis constructed from Fourier-transform infrared spectroscopy for nine samples

ysis (Figure 5B) consistently indicated that samples No. 1–6 had the highest similarity value (above 0.921). Sample No. 9 (Baise, Guangxi) had lower similarity values when compared with other samples, especially with samples No. 5 (Cenxi, Guangxi) and No. 7 (Rongxian, Guangxi): 0.735 and 0.813, respectively.

Principal component analysis of Fourier-transform infrared fingerprint of *Cinnamomum cassia* leaves. We selected the 1 800–600 cm^{-1} band for the fingerprint spectral analysis to better identify the interrelationships among the research objects and applied a PCA. As shown in Figure 6, the scatter plot was derived from the IR spectra of different samples of *C. cassia* after PCA of the principal components PC1 and PC2. The former had a variance contribution of 85.65% and was the most important component, while the latter contributed to the variance with 12.32%. The positions of the IR spectra of different *C. cassia* samples on the scatter plot corresponded to their geographical distances. Sample No. 9 (Baise, Guangxi) was notably distant from the other samples on the PC2 scatter plot, suggesting significant differences. The IR spectral characteristics of samples No. 7 and 8 (Yulin, Guangxi) were grouped, presumably due to their cultivation sites' geographical and environmental proximity.

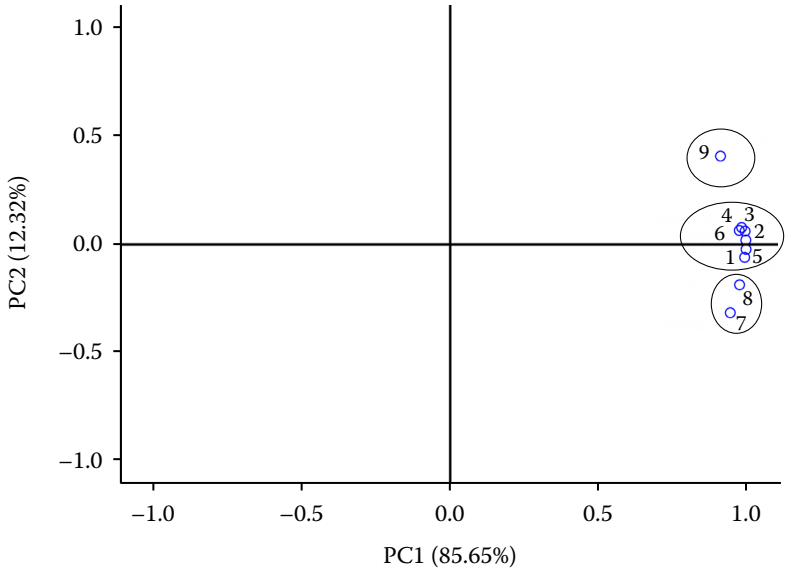

Figure 6. The scattered scores plot of infrared spectra of nine *Cinnamomum cassia* samples

PC – principal component

https://doi.org/10.17221/197/2023-CJFS

DISCUSSION

Environmental and secretory structure influences on *Cinnamomum cassia* leaf oil accumulation. Essential oil yields are influenced by climate variation, ecological environments, and growth conditions at the different cultivation sites (Li et al. 2020). The essential oil yields from nine samples of *C. cassia* leaves were significantly different in the present study. The highest yield was obtained from sample No. 5 (1.34%), followed by samples No. 6 (0.92%), No. 4 (0.89%), No. 3 (0.85%), and No. 2 (0.83%). Samples No. 7 and 8 (Rongxian County) had the lowest oil yields (0.51% and 0.55%, respectively). This variance could be attributed to factors such as climate, soil, altitude, and cultivation techniques, as well as the developmental characteristics and density of oil cells (Figueiredo et al. 2008).

Oil cells are the primary secretory structures within the cinnamon plant for the synthesis and accumulation of essential oils, and these secretory structures also influence the accumulation of the oils produced. The environment often influences the development and distribution of secretory structures. Plant volatiles is produced in specialised secretory structures that minimise the risk of autotoxicity while allowing for the presence of high levels of metabolic components where defence and/or attraction are critical (Figueiredo et al. 2008). Cen et al. (2021) reported that the thickness of the phloem affected the density of oil cells and, thus, the content of essential oil in cinnamon twigs. Similarly, oil production is closely related to the development of oil cells in cinnamon leaves (Li et al. 2013b, 2016). These results revealed that oil cell density and essential oil yield at the accumulation and saturation stages were positively correlated. For example, sample No. 5 with the highest oil cell density (4.8 $N{\cdot}mm^{-2}$) at the accumulation and saturation stages also had the highest essential oil yield (1.34%). Conversely, samples No. 7 and 8 with the lowest oil cell density (2.86 and 2.93 $N{\cdot}mm^{-2}$, respectively), yielded the least oil (0.52% and 0.55%, respectively). This confirms that essential oil yield is linked to the density of oil cells (Li et al. 2013b, 2016), which can vary with plant age, development stage, growing season, and environment (Figueiredo et al. 2008; Li et al. 2013a, b).

Geographic variation influences on the composition of *Cinnamomum cassia* leaf oil. Numerous reports indicate that the yield and composition of volatiles vary geographically, which determines the existence of different chemotypes/chemical races in some species. Thin et al. (2023) found that the composition of *Dasymaschalon rostratum* leaf oil in Vietnam was quite different from that in China. The chemical compositions of *Cinnamomum verum* can be varied depending on the geographical distribution. It has been reported that *C. verum* leaf essential oils cultivated in different regions reveal the existence of four chemotypes (eugenol, eugenol and safrole, benzyl benzoate, and linalool) (Xavier et al. 2022). Previous work revealed that yields and compositions of essential oils from cassia bark and twigs vary significantly based on their origins (Li et al. 2013a; Cen et al. 2021), which may be related to environmental conditions such as altitude, sunlight, and soil type, as well as to cultivation conditions (Figueiredo et al. 2008). In this study, the content of *trans*-cinnamaldehyde (50.36%) in sample No. 9 from Baise is significantly lower than that of the other eight samples (57.76–65.91%) near Xijiang River basin, especially of samples No. 1–6. *C. cassia*, a plant that thrives in tropical and subtropical climates, is predominantly found in the warm Xijiang River and rarely in other regions (Li and Yi 1985). The area's temperature, rainfall, and sunlight are ideal for *C. cassia*, which grows well in the prevalent acidic lateritic red soil, resulting in good-quality oil. Conversely, Baise, located in the western part of Guangxi near Yunnan province, has calcareous soil and low annual precipitation and offers a climate and environment less favorable for the growth of *C. cassia*. These factors may affect the biosynthetic pathway of plants, thus affecting the production and accumulation of *trans*-cinnamaldehyde content.

The quality standard of a single component or several components is no longer sufficient to control the overall quality of medicinal materials. FTIR fingerprinting is a comprehensive and quantifiable method to explore the complexity of medicinal materials, which can effectively reflect the comprehensive effect of the active components of medicinal materials and evaluate the quality of medicinal materials as a whole. It has been widely used in the identification of species origin and different habitats (Li et al. 2013a). The results of cluster analysis similarity analysis, and PCA based on FTIR in this study showed that samples No. 1–6 share similar climatic and soil environments due to their location in the Xijiang River basin, which is reflected in their similar chemical compositions. Obtaining medicinal plant-derived compounds is a systematic process influenced by factors such as climate, soil nutrients, and root microorganisms (Su et al. 2023). Sample No. 9 from Baise, situated in western Guangxi near Yunnan, is geographically distant from the other sampled locations. Its unique

https://doi.org/10.17221/197/2023-CJFS

climate and soil environments (calcareous soil) may contribute to the vastly different chemical composition of the corresponding oil. Localised variations in chemotype distributions were reported for thyme populations; the essential oils of *Thymus caespititius* from four populations growing just 200 m apart on S. Jorge Island, Azores exhibited significant chemical polymorphism, likely due to genetic and edaphic factors (Pereira et al. 2003). Our result indicates a strong association between the chemical composition of *C. cassia* leaf oil and cultivation regions.

CONCLUSION

GC-MS analysis demonstrated that *C. cassia* leaves from different regions have a similar abundance of *trans*-cinnamaldehyde (55.27–65.57%). However, leaves from Guangdong province had a slightly higher content of *trans*-cinnamaldehyde than those from Guangxi province, especially from the distant region of Baise, Guangxi. These results reveal the influence of the geographical environment on the essential oil yield and chemical composition of *C. cassia* leaves. By combining GC–MS and FTIR with chemometrics, the essential oil compounds were effectively classified, identified, and differentiated among the nine samples of *C. cassia* leaves, demonstrating their varying chemical compositions. The results presented herein provide a comprehensive evaluation of cinnamon quality and an optimised method for medicinal herb quality control.

REFERENCES

Bai M., Jin X., Cen Z., Yu K., Yu H., Xiao R., Deng J., Lai Z., Wu H., Li Y. (2021): GC–MS and FTIR spectroscopy for the identification and assessment of essential oil components of five cinnamon leaves. Brazilian Journal of Botany, 44: 525–535.

Błaszczyk N., Rosiak A., Kałużna-Czaplińska J. (2021): The potential role of Cinnamon in human health. Forests, 12: 648.

Cen Z.Y., Du J.H., Deng J., Lai Z.W., Yu H., Gu D.Z., Geng Z., Wu H., Li Y.Q. (2021): Volatile oil variation and morphology of Cinnamon twigs from different regions of China. Revista Brasileira de Farmacognosia, 31: 217–224.

China Pharmacopeia Commission (2020): Pharmacopoeia of the People's Republic of China. Beijing, Chinese Medical Science and Technology Press: 1–142.

Farag M.A., Khaled S.E., El, Gingeehy Z., Shamma S.N., Zayed A. (2022): Comparative metabolite profiling and fingerprinting of medicinal Cinnamon bark and its commercial preparations via a multiplex approach of GC–MS, UV, and NMR techniques. Metabolites, 12: 614.

Figueiredo A.C., Barroso J.G., Pedro L.G., Scheffer J.J.C. (2008): Factors affecting secondary metabolite production in plants: Volatile components and essential oils. Flavour and Fragrance Journal, 23: 213–226.

Jan R., Asaf S., Numan M., Kim K.M. (2021): Plant secondary metabolite biosynthesis and transcriptional regulation in response to biotic and abiotic stress conditions. Agronomy, 11: 968.

Li B.D., Yi D.H. (1985): Draft of the History of Agricultural Economy in Guangxi. Guangxi National Publishing House, Nanning: 288–289.

Li Y.Q., Kong D.X., Wu H. (2013a): Analysis and evaluation of essential oil components of Cinnamon barks using GC–MS and FTIR spectroscopy. Industrial Crops and Products, 41: 269–278.

Li Y.Q., Kong D.X., Huang R.S., Liang H.L., Xu C.G., Wu H. (2013b): Variations in essential oil yields and compositions of *Cinnamomum cassia* leaves at different developmental stages. Industrial Crops and Products, 47: 92–101.

Li Y.Q., Kong D.X., Lin X.M., Xie Z.H., Bai M., Huang S.S., Nian H., Wu H. (2016): Quality evaluation for essential oil of *Cinnamomum verum* leaves at different growth stages based on GC–MS, FTIR and Microscopy. Food Analytical Methods, 9: 202–212.

Li Y.Q., Kong D.X., Fu Y., Sussman M.R., Wu H. (2020): The effect of developmental and environmental factors on secondary metabolites in medicinal plants. Plant Physiology and Biochemistry, 148: 80–89.

Muhammad D.R., Dewettinck K. (2017): Cinnamon and its derivatives as potential ingredient in functional food – A review. International Journal of Food Properties, 20: 2237–2263.

Pereira S.I., Santos P.A., Barroso J.G., Figueiredo A.C., Pedro L.G., Salgueiro L., Deans S.G., Scheffer J.J. (2003): Chemical polymorphism of the essential oils from populations of *Thymus caespititius* grown on the islands Pico, Faial and Graciosa (Azores). Phytochemical Analysis: PCA, 14: 228–231.

Shen Y., Jia L., Honma N., Hosono T., Ariga T., Seki T. (2012): Beneficial effects of Cinnamon on the metabolic syndrome, inflammation, and pain, and mechanisms underlying these effects – A review. Journal of Traditional and Complementary Medicine, 2: 27–32.

Su J., Wang Y., Bai M., Peng T., Li H., Xu H., Guo G., Bai H., Rong N., Sahu S.K., He H., Liang X., Jin C., Liu W., Strube M.L., Gram L., Li Y., Wang E., Liu H., Wu H. (2023): Soil conditions and the plant microbiome boost the accumulation of monoterpenes in the fruit of *Citrus reticulata* 'Chachi'. Microbiome, 11: 61.

https://doi.org/10.17221/197/2023-CJFS

Thin D.B., Korneeva A.A., Thinh B.B., Ogunwande I.A. (2023): Chemical composition, antimicrobial and antioxidant activities of essential oil and methanol extract from the stems of *Dasymaschalon rostratum* Merr. & Chun. Russian Journal of Bioorganic Chemistry, 49: 815–822.

Thinh B.B., Thin D.B. (2023): Essential oil composition, antimicrobial and antioxidant properties of *Pluchea eupatorioides* Kurz collected from Vietnam. Journal of Essential Oil Earing Plants, 26: 653–663.

Xavier J.K.A.M., Baia T.G.C., Alegria V.C., Figueiredo P.L.B., Carneiro A.R., Moreira E.C.O., Maia J.G.S., Setzer W.N., Silva J.K.R. (2022): Essential oil chemotypes and genetic variability of *Cinnamomum verum* leaf samples commercialized and cultivated in the Amazon. Molecules, 27: 7337.

Yun J., Cui C., Zhang S., Zhu J., Peng C., Cai H., Yang X., Hou R. (2021): Use of headspace GC/MS combined with chemometric analysis to identify the geographic origins of black tea. Food Chemistry, 360: 130033.

Received: November 11, 2023
Accepted: May 14, 2024
Published online: June 7, 2024